BEAM-INDUCED HEATING OF THE KICKER CERAMICS CHAMBERS AT NSLS-II*

A. Blednykh†, B. Bacha, G. Bassi, G. Ganetis, C. Hetzel, H.-C. Hseuh, T. Shaftan, V. Smaluk, G. Wang, BNL, NSLS-II, Upton, NY, 11973-5000, USA

Abstract

Previous experiences with the beam-induced heating of the ceramics chambers in the NSLS-II storage ring have been discussed (reference). A total five ceramics chambers are being considered for replacement due to concerns of overheating while storing $I_{av} = 500mA$ during operations. Air cooling fans have been installed as a temporarily solution to the heating problem.

INTRODUCTION

Four ceramic chambers with titanium (Ti) coating are installed in the injection straight section (Cell 30) and one additional chamber is installed in a different straight section (Cell 22) for use with the pinger magnet. The schematic layout of the injection straight section is shown in Fig. 1. The kicker chambers have a ceramic length of 755 mm and octagonal profile of 76 mm (H) x 25 mm (V) which match the cross section of adjacent bellows and chambers. The original specification of the kicker ceramic chambers called for a 2μm thick coating of Ti- on the entire inner surface with ± 10% thickness uniformity.

The Ti-coating thickness was estimated from the end-to-end resistance measurements for each chamber. It should be noted that the measured resistance before installation and after the chamber was removed from the ring, did not change, between $R \sim 3 \div 4\Omega$. It is difficult to verify the coating thickness and uniformity along the interior surface of the chambers. Work is under way to accurately characterize these thin films.

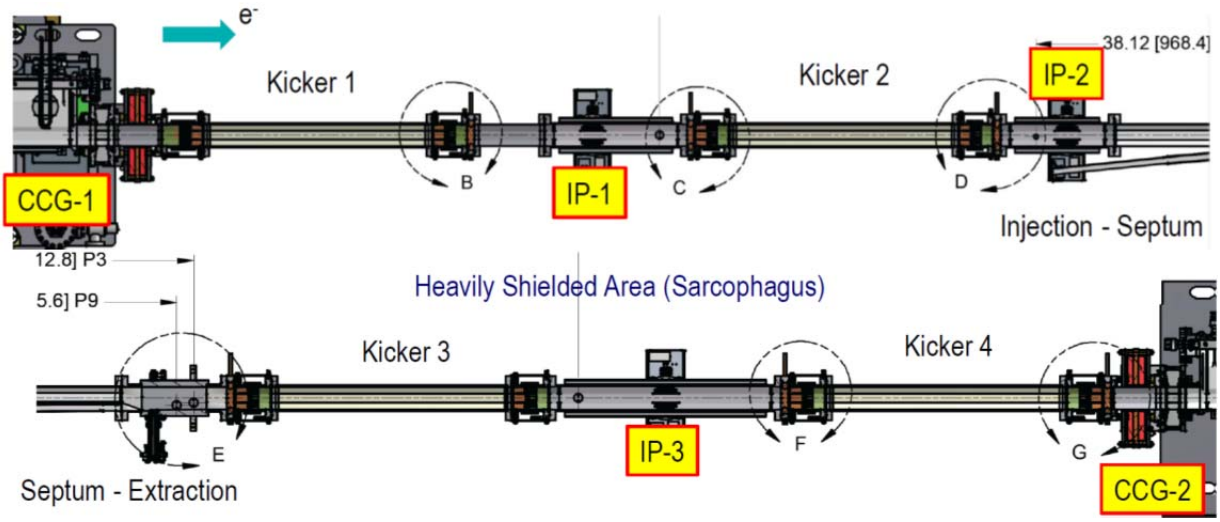

Figure 1: NSLS-II injection straight section (Cell 30).

Heating of the ceramics chambers has been observed during machine studies with an average current of $I_{av} = 375mA$ and a standard filling-pattern of $M = 1080$ bunches (Fig. 2). Several temperature RTD sensors have been installed near each transition from ceramic to stainless steel. This transition is made of Ni42 (42% of Nickel-Iron), which is used as to better match the thermal expansion of the ceramic.. It was observed that the downstream end of the kicker 2 chamber was showing a much higher temperature than the others. The maximum temperature of the Kicker2 downstream chamber as well as the other kicker chambers is shown in Fig. 2. In addition a temperature gradient was observed across the Kicker 3 chamber, $T_{3,US} \sim 75^{\circ}C$ upstream (orange trace of Fig. 2) and $T_{3,DS} \sim 55^{\circ}C$ downstream (purple trace of Fig. 2). As can be seen from Fig. 2 the temperature of the chamber had not reached steady state after one hour with $I_{av} = 375mA$ (blue trace of Fig. 2) stored in the ring. The beam current was lowered due to concern of potential damage to the resulting from the unexpected heating. During beam operation at low current, we were able to collect temperature data as a function of average current. It should be noted that, between 6-7 hours are require to reach a steady-state temperature. Figure 3, shows a plot of the temperature distribution as a function of average current. This relation appears to be quadratic fitted to a curve ($T \sim I_{av}^2$). Based on this data the heating appears to be a result of resistive wall heating rather than synchrotron radiation. Tempera-

* Work supported by Department of Energy contract DE-AC02-98CH10886
† blednykh@bnl.gov

ture data was also collected during regular operations at $V_{RF} = 1.8MV$ with $M = 1080$ bunches and one damping wiggler magnet gap closed.

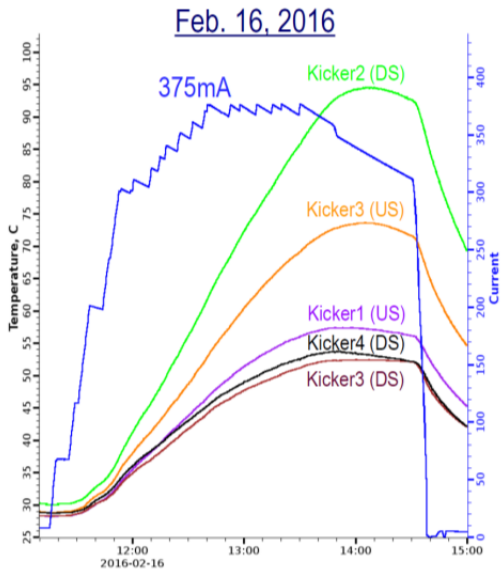

Figure 2: Temperature rise monitoring as a function of time at $V_{RF} = 1.5MV$ with $M = 1080$ bunches (Bare lattice).

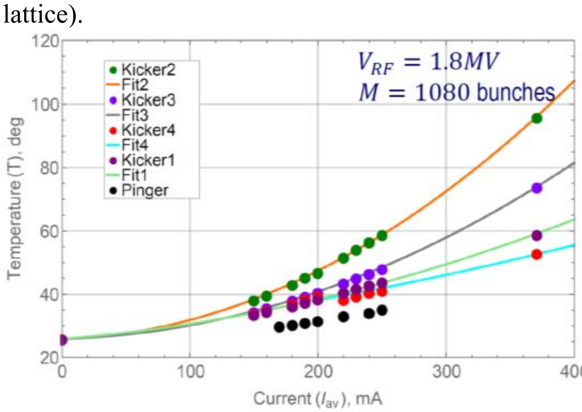

Figure 3: Temperature measurements as a function of average current. Data collected during the regular operation, except points at $I_{av} = 375mA$. Those data are preliminary, since the heat source did not reach steady state temperature.

Concerns over the excessive heating measured on the Kicker2 chamber prompted us to inspect the interior of the chamber. Once opened, the Ti-Coating found to be damaged as shown in Fig. 4. Significant colour change was also clearly apparent when compared to the spare chamber which was installed (Fig. 5). The damaged Kicker 2 chamber was replaced with the pinger chamber and spare chamber was installed in the pinger location.

To improve the heat removal, forced air cooling fans have been installed in to the kicker enclosures as a temporarily solution (Fig. 6). Figure 7 shows a side view of the pulsed magnet enclosure with cooling fans installed and air flow direction indicated.

Figure 4: Kicker 2 chamber internal view after de-installation from the storage ring. O-Ring damaged shape of Ti-coating observed at the upstream of the chamber.

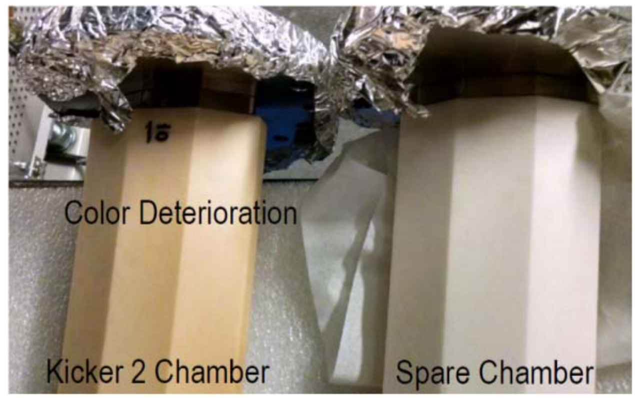

Figure 5: Comparison of the spare chamber and the Kicker2 chamber after its de-installation from the ring.

Figure 6: Cooling fans installed on the safety plastic shielding of each kicker pulse magnet.

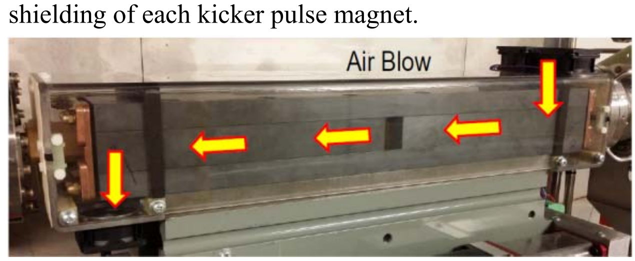

Figure 7: Side view and the schematic layout of the air flow through the kicker pulse magnet, where the ceramics chamber installed.

The newly installed cooling fans run continuously. Further experiments show that the air flow rate produced by the cooling fans is not sufficient to reduce the temperature of the upstream side of the Kicker3 chamber. To confirm that the main source of the heating is due to the resistive wall, we reduced the average current by a factor of 2 and the number of bunches by a factor of 4 (Fig. 8). Running with $I_{av} = 200mA$ in $M = 270$ bunches is similar to operation with $\boldsymbol{I_{av} = 400mA}$ in $\boldsymbol{M = 1080}$ bunches, since $T \sim I_{av}^2/M$ for beam induced heating. The bunch lengthening effect due to Potential-Well Distortion (PWD) needs to be taken into account when the intensity per bunch is large enough. Assuming small effects from PWD we compared the temperature rise for the two discussed cases.

The experiments showed a significant decrease of the chamber temperatures when the cooling fans are on. The temperature rise on all of the ceramics chambers was below $40^{\circ}C$ except for one. The upstream end of Kicker 3 showed a temperature rise up of $T_{3,US} \sim 70^{\circ}C$ with the cooling fans on during both considered cases. After two hours the temperature did not reach the steady state.

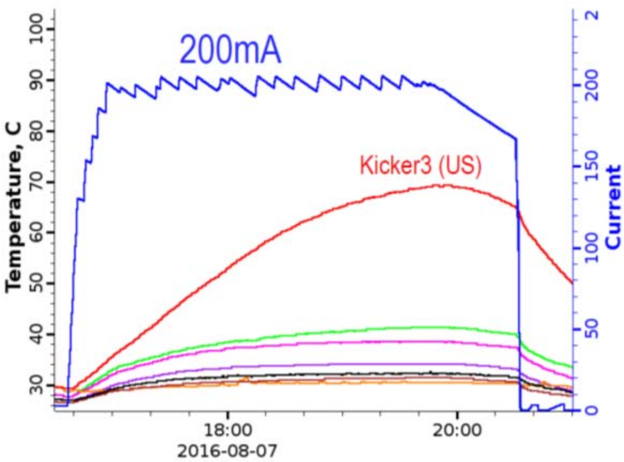

Figure 8: Beam studies at $I_{av} = 200mA$ with one train of $M = 270$ bunches.

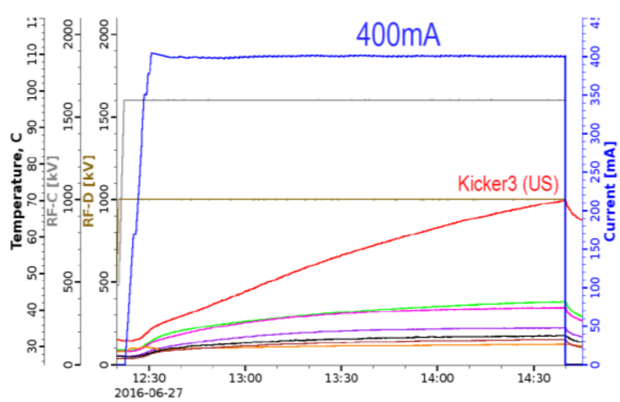

Figure 9: Beam studies at $\boldsymbol{I_{av} = 400mA}$ with one train of $\boldsymbol{M = 1080}$ bunches.

Figure 10 shows a plot of the temperature rise as a function of time for the two beam conditions described above. With some small discrepancy, the temperature effects reflect the behaviour we expected.

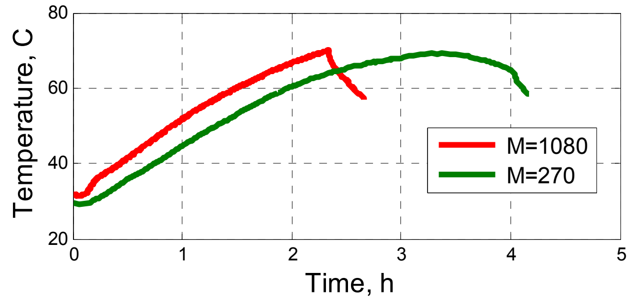

Figure 10: Temperature rise comparison as a function of time. Time is in hours. Number of bunches is M.

To understand the beam-induced heating due to resistive wall, the longitudinal impedance of the ceramic chambers has been calculated numerically using the GdfidL code [1]. Varying the electrical conductivity (σ_c) at fixed frequency, we were able to see the frequency spectrum change from broad-band resonator impedance to generation of the narrow-band impedance peaks (Fig. 11). Further decreasing the electrical conductivity makes the spectrum noisy. The loss factor (k_{loss}), estimated for a 3mm bunch length, increases with decreasing conductivity and stays constant for $\sigma_c < 1\,S/m$. To estimate the power loss accurately we need to know the electrodynamics parameters of the ceramics chamber at different frequencies and with different Ti-coating thickness.

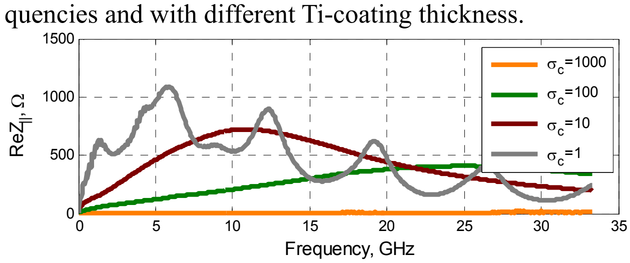

Figure 11: Real part of the longitudinal impedance simulated by the GdfidL code up to 32GHz for different electrical conductivities of the ceramics chamber.

CONCLUSION

A method to accurately measurement the Ti-coating thickness and its uniformity is under development. Five new ceramic chambers are currently being fabricated to replace the existence ones. Further work to increase the air flow and using cooled air to remove heat, is continued. Stripping and recoating the damaged chambers as well as the possibility of increasing the coating thickness on the existing chambers is being considered. Newly coated chambers will be tested under real beam conditions in one of the available straight section. Effect of the ceramics chambers on the instability thresholds and on the total impedance of the ring is currently under study.

REFERENCES

[1] W. Bruns, `http://www.gdfidl.de`